International Journal of Science and Research Archive
eISSN: 2582-8185
Cross Ref DOI: 10.30574/ijsra
Journal homepage: https://ijsra.net/

(RESEARCH ARTICLE)

Check for updates

Assessment of mechanical properties and microstructure of AA6061 reinforced with nano-sized chicken feather powder and cow-bone ash

Victor Adelegan Adewumi *, Lateef Owolabi Mudashiru and Sunday Olufemi Adetola

Department of Mechanical Engineering, Ladoke Akintola University of Technology, Ogbomosho, Nigeria.

International Journal of Science and Research Archive, 2026, 18(02), 136-145

Publication history: Received on 20 December 2025; revised on 28 January 2026; accepted on 30 January 2026

Article DOI: https://doi.org/10.30574/ijsra.2026.18.2.0177

Abstract

The demand for lightweight and sustainable engineering materials has increased interest in aluminum metal matrix composites (AMMCs) reinforced with low-cost alternatives to conventional ceramics. This study investigates the microstructural and mechanical properties of AA6061 aluminum alloy reinforced with hybrid nano-sized chicken feather powder (CFP) and cow bone ash (CBA). CFP and CBA were produced from poultry and abattoir wastes through controlled combustion and high-energy ball milling, and characterized using SEM, and EDS. Composites containing 0 to15 wt.% CFP and 0 to 2 wt.% CBA were fabricated via stir casting. Hybrid nano CFP–CBA reinforcement significantly improved mechanical performance. Hardness increased from 62 BHN for the unreinforced alloy to a maximum of 79 BHN at higher reinforcement levels, indicating enhanced resistance to plastic deformation and tensile strength reached approximately 162 MPa due to effective load transfer and grain refinement. Impact energy decreased to about 16 J with increasing reinforcement content, indicating reduced ductility, while density slightly reduced to approximately 2.69 g/cm^3. SEM analysis confirmed uniform particle dispersion and good interfacial bonding. The results demonstrate that hybrid CFP–CBA reinforced AA6061 composites offer a lightweight, low-cost, and sustainable alternative for automotive and structural applications.

Keywords: Aluminum Metal Matrix Composites (AMMS); Chicken Feather Powder (CFP); Cow Bone Ash (CBA); Nanocomposites; Sustainability

1. Introduction

Aluminium Metal Matrix Composites (AMMCs) have received considerable research attention due to their superior strength-to-weight ratio, enhanced wear resistance, good corrosion behaviour, and favourable thermal properties when compared with monolithic aluminium alloys (Kumar et al., 2021). These attributes make AMMCs attractive for applications in the automotive, aerospace, construction, oil and gas, and energy sectors, where lightweight materials with high mechanical efficiency are increasingly required. Among aluminium alloys, AA6061 is widely used as a matrix material because of its balanced mechanical performance, corrosion resistance, and excellent castability (Olawale et al., 2020).

Conventionally, AMMCs are reinforced with synthetic ceramic particulates such as silicon carbide (SiC), alumina (Al_2O_3), boron carbide (B_4C), and titanium carbide (TiC), which significantly improve hardness, tensile strength, and wear resistance (Adeniyi et al., 2023). However, these reinforcements are costly, energy-intensive to produce, and often present processing challenges, including poor wettability, particle agglomeration, and non-uniform dispersion during liquid metallurgy routes such as stir casting (Ezeh and Adekunle, 2022). These limitations restrict their large-scale adoption, particularly in developing economies, and have motivated the search for low-cost, sustainable reinforcement alternatives.

* Corresponding author: Victor Adelegan Adewumi

In response to global concerns over environmental sustainability and waste management, agro-waste and animal-waste derived materials have emerged as promising substitutes for conventional ceramic reinforcements in aluminium composites (Udo et al., 2020). Ashes derived from agro-wastes such as rice husk, coconut shell, palm kernel shell, chicken feathers, and cow bones are rich in ceramic oxides including SiO_2, Al_2O_3, CaO, MgO, and P_2O_5, which are known to contribute to strengthening, grain refinement, and improved interfacial bonding in aluminium matrices (Rahman et al., 2023).

Chicken feather powder (CFP) has gained attention as a lightweight reinforcement due to its oxide-rich composition following controlled calcination. Studies have shown that CFP contains significant amounts of CaO, SiO_2, and MgO, which promote effective load transfer and grain refinement when incorporated into aluminium alloys (Adekunle et al., 2022). When processed to the nanoscale, CFP particles exhibit a high surface-to-volume ratio, enhancing dislocation pinning and strengthening through Hall–Petch and Orowan mechanisms (Hassan et al., 2023). Similarly, cow bone ash (CBA), obtained from calcined animal bones, is rich in calcium phosphate, CaO, and MgO, making it an effective ceramic reinforcement for aluminium composites (Ibrahim et al., 2021). The presence of MgO enhances wettability between reinforcement particles and molten aluminium, improves interfacial bonding, and contributes to grain refinement and reduced porosity during stir casting (Kareem et al., 2020).

Despite these advances, existing studies largely focus on single agro-waste reinforcements, micro-scale particles, or synthetic ceramic additives. Therefore, this study investigates the development of AA6061 aluminium metal matrix composites reinforced with nano-sized chicken feather powder and cow bone ash using the stir-casting technique. The effects of hybrid CFP–CBA reinforcement on microstructure and mechanical properties including tensile strength, hardness, impact energy, and density are systematically evaluated. Microstructural characterization using scanning electron microscopy is employed to assess reinforcement dispersion and interfacial bonding.

2. Materials and Method

This section discussed the materials and methods used in this work.

2.1. Materials Procurement and Preparation

The AA6061 aluminium alloy was sourced from an aluminium company in Osogbo, Osun State, Nigeria. Chicken feathers were collected from poultry farms in Ogbomoso, Oyo State, while cow bones were obtained from an abattoir in Ile-Ife, Nigeria. The collected chicken feathers were thoroughly washed with distilled water to remove dirt and blood residues, soaked in a mild detergent solution for 15 minutes to eliminate fats and organic contaminants, and then oven-dried at 105 °C for 4 hours. The dried feathers were mechanically ground into powder and calcined in a muffle furnace at 650 °C for 2 hours to ensure complete decomposition of organic matter. The resulting ash was cooled inside the furnace, pulverized, and subsequently ball-milled for 6 hours at 200 rpm to obtain nano-sized particles as shown in Figure 1. The nano chicken feather powder (CFP) was sieved through a 200-mesh (75 μm) sieve, and particle size analysis using a Malvern Nano Zetasizer confirmed an average particle size of 70–90 nm, indicating successful nanostructuring.

Figure 1 Grinded Chicken Feather before Calcination

Cow bones were initially washed with distilled water and boiled in a 2 % sodium hydroxide solution for 30 minutes to remove residual fats and organic matter. After thorough rinsing, the bones were oven-dried at 110 °C for 6 hours and crushed into smaller fragments. Calcination was carried out in a muffle furnace at 800 °C for 5 hours, which produced Figure 2. The ash was allowed to cool naturally, gently pulverized, and ball-milled for 4 hours at 200 rpm using a ball-to-powder ratio of 10:1. The resulting cow bone ash (CBA) was sieved through a 200-mesh sieve to obtain fine particles.

X-ray fluorescence analysis confirmed CaO (48.2 wt %), P_2O_5 (28.5 wt %), and MgO (8.1 wt %) as the dominant oxides, validating its suitability as a reinforcing phase. The preparation approach is consistent with reported methods for agro-waste-derived reinforcements in aluminium matrix composites (Olanipekun et al., 2024).

Figure 2 Calcined Cow Bone Ash

2.2. Composite Formulation

The preparation of hybrid aluminum matrix composites can be carried out using a mass balance relationship to determine the weight of each constituent (Barah et al., 2025). The composite formulations used in this study are summarized in Table 1. Each batch had a total mass of 150 g. The composition was calculated using the mass balance relationship as in equation 1:

$$WT = WCFP + WCBA + WAl \quad \text{…….1}$$

2.2.1. Were

WT=total composite weight (150g), WCFP= weight of the chicken feather powder

WCBA= weight of cow bone ash, WAl = weight of the AA6061.

Table 1 Weight Distribution of Composite Percentage

Sample code	CFP (wt.%) (W_{CFP})	CBA (wt.%) (W_{CBA})	Al (wt.%) (W_{all})	Cep_{has} (g)	Cam_{ass} (g)	Al mass (g)	Total Mass (g)
N (S0)	0	0	100	0	0	150	150
B (S1)	5	1	94	7.5	1.5	141	150
C (S2)	10	1.5	88.5	15	2.25	132.75	150
D (S3)	15	2	83	22.5	3	124.5	150

2.3. Casting Process

The matrix alloy for the unreinforced control sample remained at 100 % AA6061, while for the composite samples it was maintained above 83 %, with the remaining percentage allocated to the dual reinforcements of Chicken feather powder (CFP) and Cow Bone Ash (CBA), which varied between 0 % and 17 %. According to Kareem et al. (2021), the stir casting process involves mechanical stirring of the molten aluminium alloy to create a vortex into which the reinforcement particles are introduced, ensuring a uniform particulate distribution within the matrix and excellent metallurgical bonding between the phases. This technique is widely used because of its cost effectiveness, simplicity, and proven capability to produce composites with homogeneous reinforcement dispersion.

An electric resistance furnace was used to melt the AA6061 ingots at a temperature of 750 ± 30 °C after charging into a graphite crucible. This temperature range was chosen to minimize oxidation and guarantee full melting of the matrix alloy. To remove nonmetallic contaminants and trapped hydrogen from the molten aluminium prior to reinforcement addition, Hexachloroethane (C_2Cl_4) tablets (1 % wt) were used to degas the melt. Degassing improved melt fluidity and

surface tension, promoting efficient wetting and incorporation of the reinforcement particles. The casting process and fabricated composites are shown in Figure 3 and 4 respectively.

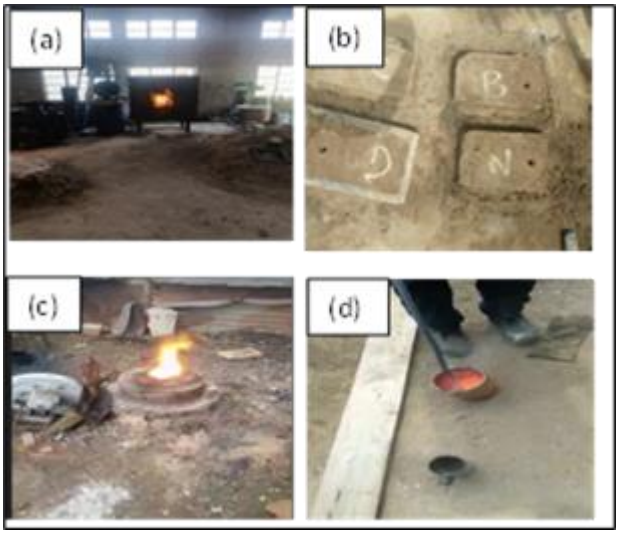

Figure 3 Casting Process

Figure 4 Fabricated Composites Sample

2.4. Morphological and Elemental Characterization

The samples for SEM examination were prepared following ASTM E1508 standard for electron microscopy analysis. Etching was performed in some cases using Keller's reagent to highlight grain boundaries and particle interfaces. Elemental composition of the samples was assessed using Energy Dispersive X-ray Spectroscopy (EDS) attached to the SEM unit. Polished specimens were exposed to an electron beam, and the characteristic X-rays emitted were analyzed to determine the elemental constituents.

2.5. Mechanical Characterization

Tensile, hardness, impact, and density tests and microstructural analysis were carried out on the composite samples. Standard specimen of dimensions 50 x 10 x 10 mm were made as a sample pieces. The tensile strength of the fabricated composites was determined using an Instron Universal Testing Machine (UTM) in accordance with the ASTM E8M-91 standard for tensile testing of metallic materials. The hardness of the composite specimens was evaluated using a Brinell Hardness Testing Machine following the guidelines of ASTM E10. A Charpy impact testing equipment was used to

evaluate the composites' impact resistance according to the requirements of ASTM E23. The mass of the control sample specimen and each composite specimen was determined using digital pioneer weighing balance and the volume was obtained by Archimedes principle. The density of each sample was calculated using equation 2.

$$\text{Density} = \frac{mass}{volume} \qquad \ldots\ldots\ldots \quad 2$$

3. Result and Discussion

The outcomes of the applied characterization methods are discussed below

3.1. Microstructure of the Composite Sample

Figures 5 present the SEM micrographs of the unreinforced aluminium alloy (Sample N) and the fabricated CFP-CBA reinforced aluminium matrix composites (Samples B, C, and D). The SEM micrographs of the aluminium matrix alloy (Figures 5a-5c) reveal a predominantly white phase, which is attributed to the α-Al matrix. This phase exhibits an equiaxed grain morphology, which is well known to contribute to favourable mechanical and physical properties such as good strength ductility balance, corrosion resistance, and electrical conductivity in aluminium alloys (Fayomi et al., 2022). In addition to the α-Al matrix, dark contrast regions are observed within the microstructure, corresponding to intermetallic constituents and oxide inclusions. These phases are typically associated with Fe-rich and Si-containing intermetallic compounds, which improve abrasion resistance and thermal stability but may act as stress concentrators if excessively coarse or unevenly distributed (Tang et al., 2021). The EDS spectra obtained from the matrix alloy confirm the presence of aluminium (Al) as the dominant element, along with oxygen (O), zinc (Zn), silicon (Si), calcium (Ca), carbon (C), and iron (Fe), indicating the presence of alloying elements and naturally formed oxide phases within the aluminium matrix.

Figures 5d to 5l show a distinct modification in microstructure due to the incorporation of CFP and CBA reinforcements. Both white and dark phases are clearly visible, where the increased dark contrast regions are associated with the ceramic reinforcement particles and their reaction products. These phases are attributed to oxides such as SiO_2, Al_2O_3, CaO, MgO, and Fe_2O_3, originating from the CFP and CBA reinforcements. The increased volume fraction of the dark phase with increasing reinforcement content confirms the successful incorporation of the ash particles into the aluminium matrix. Figures 5d and 5e (Sample B) show a fairly uniform dispersion of reinforcement particles within the matrix, with good particle-matrix interfacial bonding and limited clustering. This homogeneous distribution promotes effective load transfer across the interface and contributes to the observed improvements in hardness and tensile strength of the composite. Figure 5f further illustrates improved matrix reinforcement interaction, indicating that the processing parameters were sufficient to achieve good wetting and dispersion at this reinforcement level.

For Samples C and D (Figures 5g to 5l), a further increase in the dark phase is evident, corresponding to the higher reinforcement content. Figures 5g and 5h reveal the presence of one or two micro voids, which are likely caused by air entrapment and gas evolution during melt stirring and solidification. Such voids are common in stir-cast composites at higher reinforcement loadings and can act as crack initiation sites under impact or tensile loading (Rathod et al., 2023). Despite this, the micrographs still indicate good interfacial bonding between the aluminium matrix and the reinforcement particles, confirming the effectiveness of the two-step stir casting method adopted in this study. The presence of magnesium in the aluminium matrix played a crucial role in enhancing wettability between the molten aluminium and the ceramic reinforcements. Magnesium is known to reduce the surface tension of molten aluminium and disrupt surface oxide films, thereby promoting stronger interfacial bonding. This effect, combined with the preheating of CFP and CBA particles prior to their introduction into the melt, significantly improved particle dispersion and interface integrity (Hassan and Yusuf, 2023). The SEM micrograph in Figure 5l shows a refined microstructure with a balanced mixture of white and dark phases, free from visible cracks, severe agglomeration, or interconnected porosity.

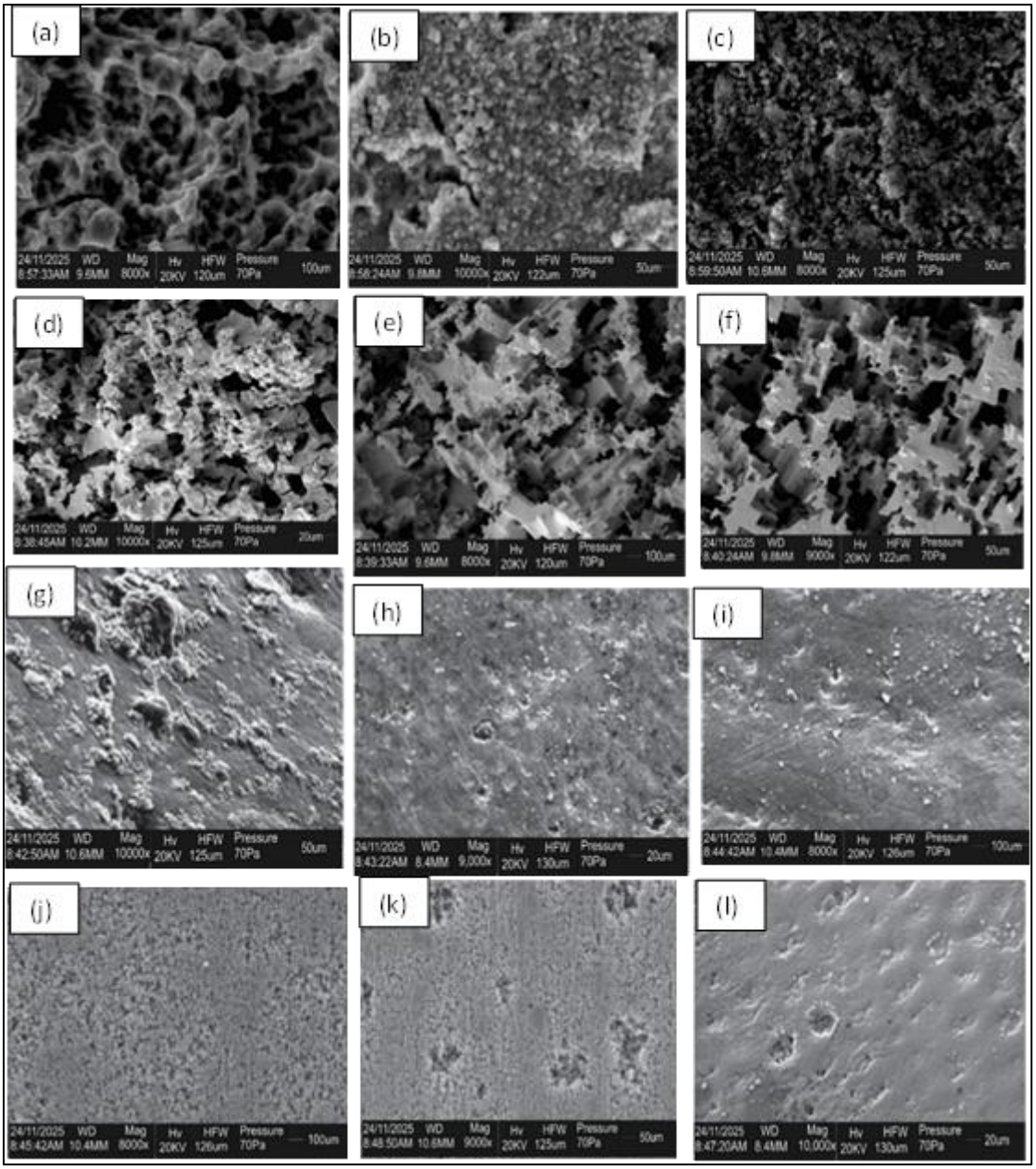

Figure 5 Scanning Electron Microscope Image of Samples

Notably, Sample D exhibits regions with excellent particle dispersion and minimal agglomeration, particularly at the particle matrix interface (Figure 5k). This suggests that optimal stirring speed, reinforcement preheating, and controlled addition contributed to improved microstructural uniformity. However, Figure 5i shows localized cavity formation, whereas Figure 5j reveals areas with little or no porosity, indicating that porosity formation was not uniform throughout the composite but depended on local processing conditions and particle distribution.

The EDS analysis of the composite samples confirms the presence of Al, Si, O, Zn, Mg, Na, Fe, Cu, Ca, and C as shown in figure 6a to 6d. These elemental peaks validate the incorporation of CFP and CBA derived ceramic phases such as silica, alumina, calcium oxide, and ferric oxides within the aluminium matrix. The combination of uniform particle distribution, grain refinement, and strong interfacial bonding explains the enhanced hardness and tensile strength observed in the composites, while the presence of occasional voids accounts for the slight reduction in impact energy at higher reinforcement contents (Alaneme et al., 2021).

Overall, the SEM and EDS analyses confirm that the CFP-CBA reinforced aluminium composites possess a well-developed microstructure, characterized by effective particle dispersion, refined grains, and strong matrix

reinforcement interfaces, demonstrating the suitability of agro-waste-derived nano-reinforcements for sustainable aluminium matrix composite development.

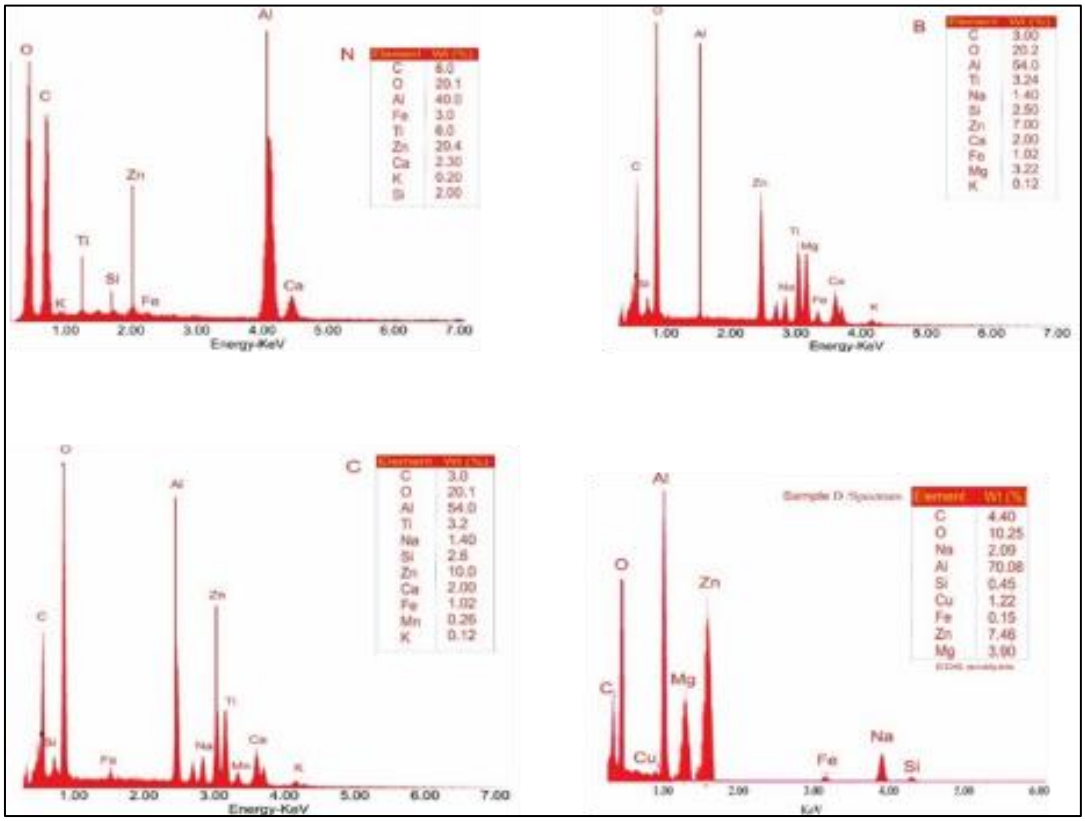

Figure 6 EDS profiles of (a) unreinforced Aluminum (b) B (S1) (c) C (S2) (d) D (S3)

3.2. Mechanical properties of composite sample

The mechanical performance of the fabricated AA6061/CFP/CBA hybrid composites was evaluated using tensile strength, Brinell hardness, impact energy, and density measurements. The results obtained from samples S0 (N), S1(B), S2(C), and S3(D) are presented, these properties provide insight into the effect of increasing reinforcement content (CFP and CBA) on the matrix alloy.

3.2.1. Density

The density of the manufactured composites was measured using the Archimedes' principle. The results are shown in Figure 7. The density of the Al 6061 alloy progressively decreases with the increasing weight percentage of the CFP and CBA reinforcements. This trend aligns with previous research on Al 6061 MMCs reinforced with other low-density agro-ashes like rice husk ash by Osumakinde et al. (2023), Olawale et al. (2025) reported that the density of AA6061-CWH composites decreased as the amount of carbonized wheat husk (CWH) increased from 0 to 15 wt%. Similarly, Fragassa and Santulli (2025) observed a density reduction when incorporating locust bean pod ash into aluminium MMCs. The decrease occurs because the ceramic ash materials (CFP and CBA) inherently possess a lower specific gravity compared to the metallic aluminium matrix material. The control sample (S0) has the highest density of 2.700 g/cm3, while the The S3 sample, incorporating the highest reinforcement load (17 wt %), exhibits the lowest density of 2.675 $g/cm3$. This decrease is primarily because the ceramic ash materials possess a lower specific gravity compared to the aluminium matrix material. The consistent reduction in density is a favorable outcome for producing lightweight components for automotive and aerospace applications. The small degree of density reduction also suggests good compaction during fabrication, minimizing significant void formation.

3.2.2. Hardness

The Brinell hardness of the composites increased steadily with increasing CFP–CBA content, as summarized in Figure 8. The unreinforced AA6061 alloy (S0) exhibited a hardness of 62 BHN, which increased to 79 BHN for the highest reinforced sample (S3). This improvement is attributed to the introduction of hard ceramic oxides (SiO_2, Al_2O_3, CaO,

and MgO) from CFP and CBA, which impede dislocation motion and enhance resistance to plastic deformation through dispersion hardening. This mechanism commonly referred to as dispersion hardening has been documented in similar works where agro-waste ashes such as rice husk ash and fly ash by Olatunji et al. (2024). Additionally, the fine ash particles acted as heterogeneous nucleation sites during solidification, promoting the formation of a refined aluminium grain structure. A finer grain structure increases the grain boundary area, which acts as additional barriers to dislocation motion, thereby increasing hardness in accordance with the Hall-Petch relationship.

3.2.3. Tensile Strength

The ultimate tensile strength (UTS) of the composites using standards such as ASTM E8/E8M, increased consistently with reinforcement content, as shown in Figure 9. The unreinforced AA6061 alloy recorded a UTS of 145 MPa, which increased to 158 MPa, 171 MPa, and 182 MPa for samples S1, S2, and S3, respectively, representing an overall improvement of up to 25.52%. This enhancement is attributed to effective dispersion of the nano-reinforcements, strong matrix particle interfacial bonding, and grain refinement induced by CFP and CBA additions. Chicken feather powder contains significant quantities of SiO_2, Al_2O_3, CaO, MgO, and K_2O, while Cow Bone Ash is rich in CaO and P_2O_5, with moderate levels of Fe_2O_3, MgO, and other oxides. These oxide phases behave similarly to conventional ceramic reinforcements such as silica, alumina, and hydroxyapatite, which are known to enhance strength by restricting dislocation motion within the matrix. When the CFP and CBA particles are introduced into the melt and effectively dispersed through stir casting, the ceramic oxide phases in the ashes act as barriers to dislocation motion and promote efficient load transfer from the aluminium matrix to the stiff reinforcement particles, consistent with dispersion strengthening mechanisms. The progressive increase in strength with reinforcement content further indicates improved interfacial bonding and a synergistic strengthening effect between CFP and CBA, in agreement with previous studies on hybrid agro-waste reinforced aluminium composites (Nguyen et al., 2022).

3.2.4. Impact Energy

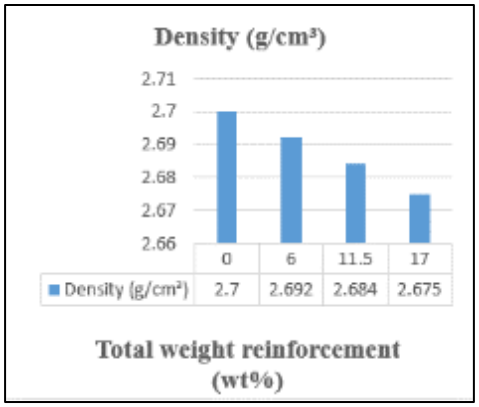

Figure 7 Chart Area Effect of Reinforcement Weight Percentage on Composite Density

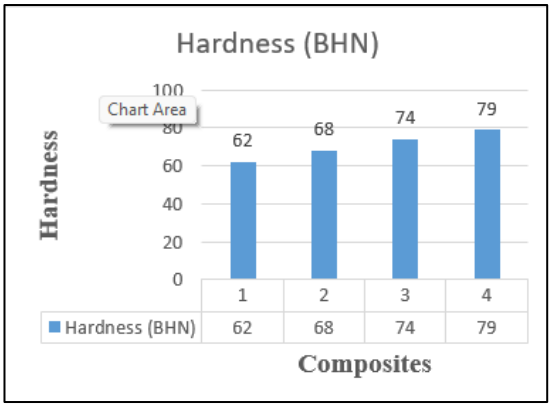

Figure 8 Effect of Reinforcement Weight Percentage on Brinell Hardness (BHN)

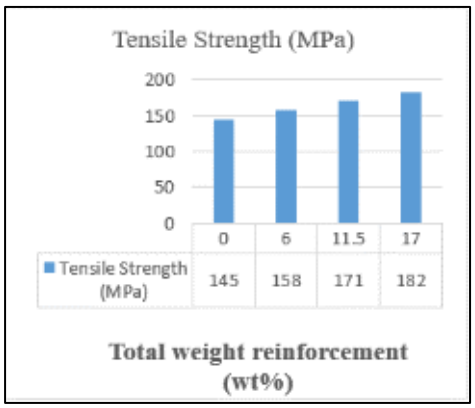

Figure 9 Effect of Reinforcement Horizontal (Category) Axis Title Percentage on Ultimate Tensile Strength (MPa)

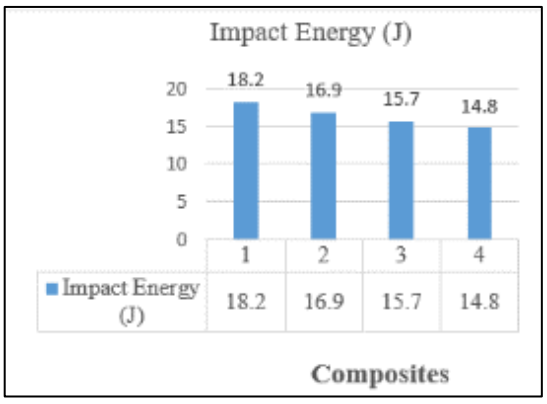

Figure 10 Effect of Reinforcement Weight Percentage on Impact Energy (J)

The impact energy of the composites decreased with increasing CFP–CBA content, as presented in Figure 10. The unreinforced AA6061 alloy exhibited the highest impact energy of 18.2 J, while reinforced samples S1, S2, and S3

recorded 16.9 J, 15.7 J, and 14.8 J, respectively, corresponding to a reduction of 7–19%. This decline is attributed to increased brittleness arising from the incorporation of hard ceramic oxides from CFP (SiO_2, Al_2O_3, CaO, MgO) and CBA (CaO, P_2O_5), which restrict plastic deformation and introduce stress concentration sites that facilitate crack initiation under impact loading. Residual stresses caused by thermal expansion mismatch between the reinforcements and aluminium matrix further contribute to reduced toughness. This strength–toughness trade-off is consistent with observations reported for agro-waste reinforced aluminium composites (Fayomi et al., 2022).

4. Conclusion

This study demonstrated the feasibility of utilizing agro-waste–derived nano-reinforcements, specifically chicken feather powder (CFP) and cow bone ash (CBA), in the development of AA6061 aluminium metal matrix composites. Characterization results confirmed that both CFP and CBA contain ceramic oxide phases suitable for reinforcement, and their successful conversion to nano-scale particles enhanced their effectiveness within the aluminium matrix. Hybrid nano CFP–CBA reinforced composites were successfully fabricated using the stir-casting technique, producing sound castings with good interfacial bonding and relatively uniform particle distribution, thereby reaffirming stir casting as a cost-effective and scalable fabrication route.

Mechanical testing revealed significant improvements in hardness and tensile strength with increasing reinforcement content compared to the unreinforced alloy, attributed to grain refinement, dispersion strengthening, and efficient load transfer. However, a reduction in impact energy at higher reinforcement levels highlighted the inherent strength–toughness trade-off associated with ceramic reinforcements. Microstructural analysis using SEM and EDS confirmed good particle dispersion and interfacial integrity, which strongly correlated with the observed mechanical performance.

Overall, the results confirm that hybrid nano CFP–CBA reinforcements provide a sustainable and technically viable approach for enhancing the performance of aluminium matrix composites, particularly for applications requiring improved strength and wear resistance.

Future work should focus on optimizing reinforcement combinations and processing parameters using statistical design tools, as well as conducting extended mechanical, tribological, and corrosion studies to assess long-term service performance. Additionally, scale-up studies, cost–benefit analysis, and environmental impact assessments are recommended to support the industrial adoption of agro-waste-based aluminium composites.

Compliance with ethical standards

Disclosure of conflict of interest

The authors declare that there is no conflict of interest regarding the publication of this article

References

[1] Adekunle, A. A. (2022). Evolution of metal matrix composites for engineering applications. Materials Science Forum, 1054, 112-121.

[2] Adeniyi, A. A., Salawu, E. Y., and Lawal, S. A. (2023). Processing, microstructural evolution and mechanical behaviour of aluminium matrix composites reinforced with ceramic particulates. Journal of Materials Engineering and Performance, 32(7), 2984-2996.

[3] Alaneme, K. K., Ikubanni, P. P., and Oladele, I. O. (2021). Mechanical and tribological behaviour of aluminium matrix composites reinforced with agro-waste ashes. Journal of Materials Research and Technology, 14, 1854-1865

[4] Barah, O. O., Onyelowe, K. C., Nnamchi, S. N. (2025). Microstructure and toughness characterization of AA6061 hybrid composite reinforced with eucalyptus ash, periwinkle shell, and plantain fiber. Discover Applied Sciences, 7, Article 202. https://doi.org/10.1007/s42452-025-06532-1

[5] Ezeh, J. C., and Adekunle, A. A. (2022). Nano-scale reinforcement strategies for aluminium alloys using bio-derived materials. Materials Today: Proceedings, 62, 4503-4510.

[6] Fayomi, O. S. I., Sojobi, J. W., Nkiko, M. O., Akande, I. G., and Noiki, A. A. (2022). An overview of the influence of agro waste reinforcement on aluminium matrix composites. In AIP Conference Proceedings (Vol. 2437, No. 1, p. 020123). AIP Publishing LLC.

[7] Fragassa, C., and Santulli, C. (2025). Hybridization of Lignocellulosic Biomass into Aluminum-Based Materials: Comparing the Cases of Aluminum Matrix Composites and Fiber Metal Laminates. Journal of Composites Science, 9(7), 356.

[8] Hassan, S. B., Afolabi, A. S., and Kareem, B. (2023). Nano-reinforced aluminium composites fabricated from agro-waste ashes. Journal of Materials Research and Technology, 25, 1345-1360.

[9] Kareem, B., Hassan, S. B., and Afolabi, A. S. (2020). Influence of magnesium on interfacial bonding in aluminium composites. Journal of Materials Engineering and Performance, 29(3), 1720-1728.

[10] Kumar, N., Prakash, J., and Singh, R. (2021). Aluminium metal matrix composites: A review of recent developments. Materials Today: Proceedings, 44(1), 189-196.

[11] Nguyen, T. T., Tran, P. T., and Hoang, V. H. (2022) Effect of nano-ceramic reinforcement on aluminium matrix composites. Materials Research Express, 9(8), 085308.

[12] Olanipekun, K. A., Ojo, A. A., and Lawal, A. S. (2024). The effect of cow bone particulate on the mechanical properties and the microstructure of aluminium brass. International Journal of Research and Scientific Innovation, 11(10), 348–354.

[13] Olatunji, P. A., Khoathane, M. C., and Washington, W. (2024). Mechanical and microstructural characteristics of recycled aluminium matrix reinforced with rice husk ash. AIMS Materials Science, 11(5), 918-934. https://doi.org/10.3934/matersci.2024044

[14] Olawale, O. O., Afolabi, A. S., and Hassan, S. B. (2020). Mechanical response of AA6061 reinforced with bio-derived particulates. Materials Research Express, 7(8), 085301.

[15] Rahman, M. M., Hassan, S. B., and Kareem, B. (2023). Hybrid nano-reinforced aluminium composites produced via stir casting. Journal of Materials Research and Technology, 24, 410-425.

[16] Rathod, Barman, A., Biswas, A., A., and Singh, M. (2022). A review paper on development of aluminum matrix composite with organic reinforcements. International Journal for Research in Applied Science and Engineering Technology, 10(10).

[17] Tang, J. J., Yu, F. L., Zhang, H. H., and Chen, D. (2021). Effect of microstructure refining on the thermal stability and wear resistance of abradable AlSi-polyester coating. Journal of Thermal Spray Technology, 30(6), 1615-1623.

[18] Udo, G. J., Okafor, E. G., and Hassan, S. B. (2020). Mechanical behaviour of aluminium matrix composites reinforced with agro-waste ashes. Materials Research Express, 7(9), 095303.